

European Centre
for Medium Range
Weather Forecasts

**Numerical Tests of Parameterisation
Schemes at an Actual Case of
Transformation of Arctic Air**

**Internal Report 10
Research Dept.**

June 1977.

Centre Européen pour les Prévisions Météorologiques
à Moyen Terme

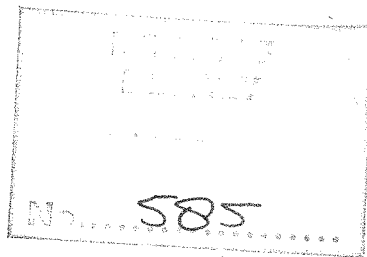
Europäisches Zentrum Für Mittelfristige Wettervorhersagen

Numerical tests of parameterisation
schemes at an actual case of
transformation of arctic air

by

Michael Tiedtke

European Centre for Medium Range Weather Forecasts, Bracknell



NOTE:

This paper has not been published and should be regarded as an Internal Report from ECMWF Research Department.

Permission to quote from it should be obtained from the Deputy Director, Head of Research, at ECMWF.



A B S T R A C T :

A case of transformation of arctic air when being advected over the sea is used in order to test different parameterisation schemes (two convective schemes and two boundary layer flux formulations). The numerical experiments show for this special case that the predicted air mass changes agree better with the observed ones when

- a) the dry adiabatic mixing which is generally applied only to sensible heat is also applied to moisture and momentum and when
- b) the moist adiabatic adjustment scheme is replaced by the convection scheme proposed by KUO (1965) which gives heating and moistening of the air up to a considerably larger height compared to the former one.

The two schemes for the surface flux calculations, i.e.

- i) the scheme used in the GFDL-model with a drag coefficient $C_d = 1.3 \cdot 10^{-3}$ and
- ii) a scheme recently proposed by LOUIS (Internal Report 4)

give about the same values for the surface fluxes of sensible heat and moisture.

1. Introduction

During the last few years considerable efforts have been made to improve the parameterisation of physical processes in numerical models. As these schemes are designed for models which simulate either very long range atmospheric processes (general circulation) or rather short range processes (cloud development, hurricanes), it is uncertain which of these schemes are most suitable for medium range weather prediction models. It is likely that definite conclusions cannot be drawn unless actual forecasts are performed with different sets of parameterisation schemes. However, synoptic changes are generally caused by many processes being active simultaneously and interacting among themselves. It will be very difficult, therefore, to make reliable decisions as to whether one distinct process is parameterised well.

Parameterisation schemes can be better examined perhaps by performing experiments for selected cases where the synoptic changes are determined mainly by those processes to be examined and where others can be neglected. One example suitable for examining the boundary-layer flux formulation and the convective scheme is the transformation of an arctic air mass being advected over the warmer sea. One case of such an air mass transformation has recently been investigated by ØKLAND (1976). This case has been used in this study to test the parameterisation of convective fluxes and of the surface fluxes of heat and moisture.

Though the air mass is being transformed rather rapidly (during 18 hrs. in this case) it is believed that this air mass transformation is important for longer term development and must therefore be well predicted in medium range weather prediction models.

2. A Case of Air Mass Transformation

The parameterisation schemes described later are tested at an example of outbreak of arctic air over the Norwegian Sea and Northern Scandinavia, investigated and described by ØKLAND (1976). Figure 1 shows the surface weather analysis for November 21, 1975, 12 GMT. At Björnøya the temperature is -15°C , but when the air is advected over the warmer sea (Figure 2) it is heated and the temperature is increased to nearly 0°C at the north coast of Norway. Figure 3 shows two soundings drawn in a skew T-log p diagram. The warmer sounding is taken from Bodø at the same time as the surface map in Figure 1, while the other refers to Björnøya 12 hours earlier (solid lines for temperatures and broken lines for dewpoints in Fig. 3). As pointed out by ØKLAND the wind field is rather stationary over the whole area with little vertical wind shears. Therefore it seems justified to assume that the air is moving horizontally from Björnøya southwards without significant internal deformations.

The temperature and humidity changes are then presumably caused only by fluxes of sensible and latent heat from the sea surface. Comparison of the soundings at Bjornøya and Bodø gives an increase of sensible heat by

$$\Delta H = \frac{c_p}{g} \int_{p'}^{p_0} (T_2 - T_1) dp = 25.10^6 \text{ Jm}^{-2}$$

and an increase of latent heat by

$$\Delta W = \frac{L}{g} \int_{p'}^{p_0} (q_2 - q_1) dp = 5.10^6 \text{ Jm}^{-2}$$

where p' is 700 mb and where T_1, q_1 and T_2, q_2 refer to Bjørnøya and Bodø, which are regarded as endpoints of a trajectory for air moving southwards in 18 hours (these figures are taken from ØKLAND's paper). Since cumulonimbus clouds and precipitation are reported from all of the coastal stations in Norway the total heating and moistening is caused by turbulent fluxes taking place within the boundary layer and also by convective motion.

In our model only these two processes are therefore included, while others such as radiation and advection are neglected

The air mass transformation is therefore simulated in a one grid point model, where the surface temperature increases with time as is specified in Figure 2.

3. Parameterisation of Convection

3.1 Dry convection

Two schemes have been tested, namely

- a) the dry adiabatic adjustment scheme and
- b) a diffusion type scheme.

3.1.1 Dry adiabatic adjustment (DAD)

This scheme which is generally used in forecast models works as follows :

The adjustment takes place whenever the stratification is superadiabatic. The adjustment is made so that the stratification becomes adiabatic. During the adjustment process the sum of internal plus potential energy is conserved.

If for instance the stratification between two vertical layers is unstable

$$\theta_k < \theta_{k+1}, \quad (1)$$

the new state becomes $\theta_k^N = \theta_{k+1}^N$ or

$$\theta_k + \Delta T_k \left(\frac{p_0}{p_k} \right)^{R/c_p} = \theta_{k+1} + \Delta T_{k+1} \left(\frac{p_0}{p_{k+1}} \right)^{R/c_p} \quad (2)$$

The temperature changes ΔT_k and ΔT_{k+1} made are related by the energy equation

$$\Delta T_k \Delta \sigma_k = - \Delta T_{k+1} \Delta \sigma_{k+1} \quad (3)$$

3.1.2 Dry adiabatic diffusion (DRYDIFF)

The dry adjustment scheme works only on the temperature field. In order to include also momentum and moisture fluxes, (2) and (3) are simulated as diffusion terms. The diffusion coefficient resulting thereby may then be used in corresponding diffusion terms for moisture and momentum.

From (2) and (3) we get

$$\Delta T_{k+1} = - \frac{\theta_{k+1} - \theta_k}{\Delta \sigma_{k+1} \left(\frac{1}{\Delta \sigma_{k+1}} \left(\frac{p_0}{p_{k+1}} \right)^{R/c_p} + \frac{1}{\Delta \sigma_k} \left(\frac{p_0}{p_k} \right)^{R/c_p} \right)}$$

$$\Delta T_k = \frac{\theta_{k+1} - \theta_k}{\Delta \sigma_k \left(\frac{1}{\Delta \sigma_{k+1}} \left(\frac{p_0}{p_{k+1}} \right)^{R/c_p} + \frac{1}{\Delta \sigma_k} \left(\frac{p_0}{p_k} \right)^{R/c_p} \right)}$$

Since similar equations hold for the adjacent layer k-1 the complete temperature change at k- level, written down in the usual notation, becomes

$$\Delta T_k = \left[\delta_\sigma \left[\gamma \Delta \sigma \frac{\delta_\sigma \theta}{\frac{2}{\Delta \sigma} \left(\frac{p_0}{p} \right)^{R/c_p} \sigma} \right] \right] \quad (4)$$

where

$$\gamma = \begin{cases} 1 & \text{for unstable layers} \\ 0 & \text{for stable layers} \end{cases}$$

The diffusion terms used for moisture and momentum in this study are

$$\Delta q = \delta_{\sigma} \left(\gamma \sigma \frac{\delta_{\sigma} q}{\left[\frac{1}{\Delta \sigma} \right]^{\sigma}} \right) \quad (5)$$

$$\Delta W = \delta_{\sigma} \left(\gamma \sigma \frac{\delta_{\sigma} W}{\left[\frac{1}{\Delta \sigma} \right]^{\sigma}} \right)$$

where again $\gamma = 1$ for unstable layers and $\gamma = 0$ for stable layers.

3.2 Moist Convection

3.2.1 Moist adiabatic adjustment (MANABE)

This scheme proposed by MANABE et al (1965) and used in the GFDL-model works like the dry adiabatic adjustment except that now the latent heat release is taken into account. The adjustment is made for an air column which

- a) is saturated everywhere ($f \geq 100\%$) and which
- b) is moistadiabatically unstable stratified

$$\frac{\partial T}{\partial \sigma} > \Gamma_e, \quad \Gamma_e = \frac{RT}{c_p T} \frac{p + \frac{0.622}{RT} L e_s}{p + \frac{0.622}{c_p} L \frac{\partial e_s}{\partial T}}$$

(L = latent heat, e_s = saturation water vapour pressure).

During the adjustment process the total energy of the air column is assumed to be conserved

$$\int_{\sigma_T}^{\sigma_B} (c_p \Delta T + L \cdot \Delta q) d\sigma = 0,$$

where the indices T and B denote top and bottom of the column in question.

After the adjustment has been made the stratification is moistadiabatic

$$\frac{\partial T^N}{\partial \sigma} = \Gamma_e(T^N, q^N)$$

$$q^N = q_s(T^N)$$

(N denoting the new state).

There are two disadvantages of this scheme. The first one is the saturation criterion which allows convection to occur only in saturated air whereas it is well known that moist convection occurs also in non-saturated air. Secondly, this scheme may cause numerical problems as the adjustment takes place instantaneously. When the criterion for moist convection is met in the model the adjustment is done completely and gives probably large temperature changes. These changes cause geostrophic imbalances and also two grid waves when the adjustment is to be done at one grid point but not at the neighbouring grid points.

3.2.2 The KUO-scheme

This scheme which was designed by KUO (1965,1974) for parameterising deep convection in tropical regions has also been used here.

The criteria for the occurrence of moist convection are :

- a) conditionally unstable stratification and
- b) vertically integrated moisture accession due to large-scale moisture convergence plus evaporation from the surface.

In case that a) and b) are valid cumulus cloud air is assumed to be created by lifting surface air. The cloud base is the lifting condensation level of the surface air and the top is where the moist adiabat meets the environmental temperature profile through this condensation level. The amount of cloud air that is generated is assumed to be equal to the accession of moisture. The generated cloud air exists only momentarily and is completely dissolved by mixing with the environmental air.

The amount of moisture assessment is just equal to the surface moisture flux

$$I = (F_q)_0 \tag{6}$$

where F_q is the assessment of moisture due to turbulent fluxes in the air column from the surface ($\sigma = 1$) to the top of the clouds.

All this accession goes into making the surplus of total energy of the cloud air against the environment. The surplus per unit square is

$$p = \frac{p_s \sigma}{g} \int_{\sigma_{\text{Top}}}^{\sigma_{\text{Bot}}} (c_p(T_c - T) + L(q_c - q)) d\sigma \quad (7)$$

where T_c, q_c define the cloud and T, q the environment. The fractional area which is produced by the accession of moisture then follows from

$$L I = \alpha p \quad (8)$$

The heating and moistening of the air after mixing the cumulus air with the environmental air give the new values for T and q as

$$\begin{aligned} T^N &= T + \alpha(T_c - T) \\ q^N &= q + \alpha(q_c - q) \end{aligned} \quad (9)$$

4. Parameterisation of Turbulent Fluxes

The parameterisation of the turbulent fluxes is performed as in the GFDL-model. Besides the original version a modified version is also used, where the surface flux calculation is changed in order to let the fluxes depend on stability and surface roughness.

4.1 Surface fluxes

Two schemes are used:

1. The GFDL-scheme, where the drag coefficient is constant (independent of stability)
2. A more sophisticated scheme, designed by J.F. LOUIS(1977) where the fluxes depend on stability and on surface roughness.

4.1.2 GFDL-scheme

The surface fluxes for momentum τ_0 , sensible heat $(F_H)_0$ and moisture $(F_q)_0$ are specified by

$$\begin{aligned} \tau_0 &= + \rho_h C_d |W_h| W_h \\ (F_H)_0 &= \rho_h c_p C_d |W_h| (\theta_o - \theta_h) \\ (F_q)_0 &= \rho_h C_d |W_h| (q_s(T_o) - q_h) \end{aligned} \quad (10)$$

where h and 0 refer to the lowest level in the model and to the surface, $q_s(T_o)$ is the saturation mixing ratio at $T = T_o$ and ρ is the density. The drag coefficient C_d is assumed constant.

$$C_d = 1.3 \cdot 10^{-3}. \quad (11)$$

This value is most suitable for the measurements over the sea. (AUGSTEIN(1976)).

4.1.2 LOUIS-scheme

This scheme being proposed by LOUIS (1977) takes into account the effects of stability and of surface roughness on the surface fluxes. The fluxes are determined as follows :

Unstable case ($\theta_h < \theta_o$)

$$\tau_o = \rho_h a \left[|W| - \frac{bx}{|W| + abc_m \left(\frac{h}{z_o}\right)^{\frac{1}{2}} |x|^{\frac{1}{2}}} \right] W$$

$$(F_H)_o = \rho_h \frac{a}{P} \left[|W| - \frac{bx}{|W| + abc_h \left(\frac{h}{z_o}\right)^{\frac{1}{2}} |x|^{\frac{1}{2}}} \right] (\theta_o - \theta_h) \quad (12)$$

$$(F_q)_o = \rho_h \frac{a}{P} \left[|W| - \frac{bx}{|W| + abc_h \left(\frac{h}{z_o}\right)^{\frac{1}{2}} |x|^{\frac{1}{2}}} \right] (q_s(T_o) - q_h)$$

with $x = \frac{gh}{\theta_h} (\theta_o - \theta_h)$

Stable case ($\theta_h > \theta_o$)

$$\tau_o = \rho_h a \left(1 - \frac{bx}{2|W| \frac{z}{h}}\right)^2 |W|_h^2 W_h$$

$$(F_H)_o = -\rho_h \frac{a}{P} \left(1 - \frac{bx}{2|W| \frac{z}{h}}\right)^2 |W|_h^2 (\theta_o - \theta_h)$$

$$(F_q)_o = -\rho_h \frac{a}{P} \left(1 - \frac{bx}{2|W| \frac{z}{h}}\right)^2 |W|_h^2 (q_o - q_h) \quad (13)$$

for $gh \frac{\theta_o - \theta_h}{\theta_h^2 |W|_h^2} < \frac{2}{b}$

and

$$(F_H)_o = (F_q)_o = 0 \quad (14)$$

$$\text{for } gh \frac{\theta_o - \theta_h}{\theta_h^2 |V|_h^2} \geq \frac{2}{b}$$

The numerical values for the parameters are

$$a = k^2 / \left(\ln \frac{h}{z_o} \right)^2 \text{ with } k = 0.35$$

$$b = 9.4, \quad P = 0.74, \quad C_m = 7.4., \quad C_h = 5.3$$

This scheme needs values for the surface roughness z_o , which is calculated in the model by using the CHARNOCK formula

$$z_o = a \frac{U_*^2}{g} \text{ with } U_*^2 = \tau_o / P_h \quad (15)$$

where $a = 0.032$ (CLARKE(1970)) and

$$\rho_o U_*^2 = |\tau|_o .$$

4.2 Turbulent Fluxes above the Surface Layer

Above the surface layer the fluxes are calculated as in the GFDL model: The fluxes of momentum and moisture are calculated by

$$\tau = \rho K \frac{\partial W}{\partial z}$$

$$F_q = -\rho K \frac{\partial q}{\partial z}$$

where

$$K = \ell^2 \left| \frac{\partial W}{\partial z} \right|$$

and the mixing length is specified by

$$\ell = k_o \cdot h \frac{H - z}{H - h} \text{ for } h \leq z \leq H$$

$$\ell = 0 \text{ for } z > H$$

($H = 2.5$ km, $k_o = 0.4$).

The turbulent fluxes of sensible heat are neglected in the model.

5. Model Equations

The equations used in this study are :

$$\begin{aligned} \frac{\partial v}{\partial t} &= f [kX(v_g - v) - \frac{g}{p_*} \frac{\partial \tau}{\partial \sigma} + (F_M)_{DC} \\ \frac{\partial T}{\partial t} &= \frac{g}{p_*} \frac{\partial H}{\partial \sigma} + (F_H)_{DC} + (F_H)_{MC} + \frac{L}{c_p} C \\ \frac{\partial q}{\partial t} &= \frac{g}{p_*} \frac{\partial W}{\partial \sigma} + (F_q)_{DC} + (F_q)_{MC} - C \end{aligned} \quad (17)$$

where C is the condensation rate of water vapour and

$$(F_M)_{DC}, (F_H)_{DC}, (F_H)_{MC}, (F_q)_{DC}, (F_q)_{MC}$$

are the source terms for momentum, sensible heat and water vapour due to dry convection and to moist convection, respectively. ($p_* = 1010$ mb, $\sigma = p/p_*$)

6. Results

The numerical experiments performed are specified schematically in table 1. Various combinations of the different parts of the parameterisation scheme have been tried. The results of the performed runs are shown in fig. 4 - 8 together with the initial state and also with the observed state and in table 2 which summarises the results of the budget calculations for sensible and latent heat ($\Delta H, \Delta W =$ predicted changes of sensible and latent heat content, respectively; $(F_H)_0, (F_W)_0 =$ surface fluxes of sensible and latent heat; $(\Delta H)_{COND}, (\Delta H)_{MC} =$ changes of sensible heat content due to condensation by supersaturation and by convection).

As is seen from fig. 4 - 8 predicted and observed soundings differ most for runs 1 - 3 (run 1 is not plotted here, since it is nearly identical to run 2) but agree much better for the later runs 3 - 6. This is specially true for the dew point soundings and is less pronounced for the temperature soundings, showing a 10 to 20% larger heating in runs 4 - 6 compared with runs 1 - 3.

TABLE 1 : Schematic description of the various runs

RUN	DRY CONVECT.	MOIST CONVECT.	SURF. FLUX CALCUL.
1	DAD	NO	GFDL
2	"	MANABE	"
3	"	KUO	"
4	DRYDIFF	MANABE	"
5	"	KUO	"
6	"	KUO	LOUIS

TABLE 2 : Diagnostics for the various runs
(units are 10^6 J/m²)

RUN	ΔH	ΔW	$(F_H)_o$	$(F_W)_o$	$(\Delta H)_{COND}$	$(\Delta H)_{MC}$
1	15.3	3.4	11.2	7.5	4.1	-
2	15.9	3.5	11.8	7.6	0.6	3.5
3	16.2	3.8	11.8	8.2	2.0	2.4
4	17.9	5.3	13.1	10.1	3.6	1.2
5	19.7	5.2	13.9	11.0	1.1	4.7
6	20.5	5.2	16.0	9.7	1.7	2.8
obs.	25	5	-	-	-	-

The earlier runs 1 - 3 differ from the later ones 4 - 6 mainly with regard to the dry adiabatic mixing used. In runs 1 - 3 dry adiabatic mixing is applied only to sensible heat, whereas in runs 4 - 6 it is also applied to moisture. The results demonstrate clearly that neglect of the dry adiabatic mixing of moisture can lead to considerable errors even in cold air where the moisture content is rather small.

Different results are also obtained for those runs which differ only in the moist convection scheme. The runs 3 and 5 with the KURO convection scheme (fig. 5 and fig. 7) give heating and moistening of the air up to a considerably larger height compared with the runs 2 and 4 with the MANABE scheme (fig. 4 and fig. 6). The KURO-runs therefore yield more realistic soundings of temperature and dew-point. The surface fluxes of sensible and latent heat are also somewhat larger in the KURO runs, though the total heating and moistening is still smaller than observed. Run 5 and run 6 are made in order to test the surface flux formulation being proposed by LOUIS(1977). By comparing fig. 7 and fig. 8 it may be seen that the use of the LOUIS-scheme gives a further improvement, as the soundings of temperature and dew-point get closer to the observed soundings. However, it must be mentioned that the LOUIS-scheme is far more sophisticated than the GFDL-scheme and is, therefore, far more expensive. Considering this increased computational amount, we may say that run 5 with the simple GFDL-version already gives reasonable results. However, this is partly due to the fact that a realistic value for the drag coefficient C_d has been pre-assigned ($C_d = 1.3 \cdot 10^{-3}$). This value is rather close to the value which resulted from the LOUIS-scheme ($C_d = 1.14 \cdot 10^{-3}$).

References :

- Augstein, E. (1976) Boundary layer observations over the oceans. Seminars on the treatment of the boundary layer in numerical weather prediction, Reading 6 - 10 September 1976.
- Clarke, R.H. (1970) Recommended methods for the treatment of the boundary layer in numerical models. Austr. Met. Magaz. Vol. 18, pp. 51 - 71
- Louis, J.F. (1977) Parameterisation of the surface fluxes. Internal Report 4, Research Dept. E.C.M.W.F.
- Manabe, S. (1965) Simulated climatology of a general circulation model with a hydrological cycle. M.W.R. 93, pp.769 - 797.
- Smagorinsky, J. and Strickler, R.F.
- Kuo, H.L. (1965) On the formation and intensification of tropical cyclones through latent heat release by cumulus convection. J.A.S. 22, pp. 40 - 63
- Kuo, H.L. (1974) Further studies of the parameterisation of the influence of cumulus convection on large-scale flow. J.A.S. 31, pp. 1232 - 1240
- Økland, H. (1976) An example of air-mass transformation in the arctic and connected disturbances of the wind field. Report DM-20, University of Stockholm.
- Smagorinsky, J. et al (1976) Numerical results from a nine-level general circulation model of the atmosphere. M.W.R. 93, pp.727 - 768.

EUROPEAN CENTRE FOR
MEDIUM RANGE WEATHER
FORECASTS

Research Department (RD)

Internal Report No. 10

- No. 1 Users Guide for the G.F.D.L. Model
(November 1976)
- No. 2 The Effect of Replacing Southern Hemispheric
Analyses by Climatology on Medium Range
Weather Forecasts
(January 1977)
- No. 3 Test of a Lateral Boundary Relaxation Scheme
in a Barotropic Model
(February 1977)
- No. 4 Parameterisation of the surface fluxes
(February 1977)
- No. 5 An Improved Algorithm for the Direct Solution of
Poisson's Equation over Irregular Regions
(February 1977)
- No. 6 Comparative Extended Range Numerical Integrations
with the E.C.M.W.F. Global Forecasting Model
1: The N24, Non-Adiabatic Experiment
(March 1977)
- No. 7 The E.C.M.W.F. Limited Area Model
(March 1977)
- No. 8 A Comprehensive Radiation Scheme designed for
Fast Computation
(May 1977)
- No. 9 Documentation for the E.C.M.W.F. Grid Point Model
(May 1977)
- No.10 Numerical Tests of Parameterisation Schemes at an
Actual Case of Transformation of Arctic Air
(June 1977)

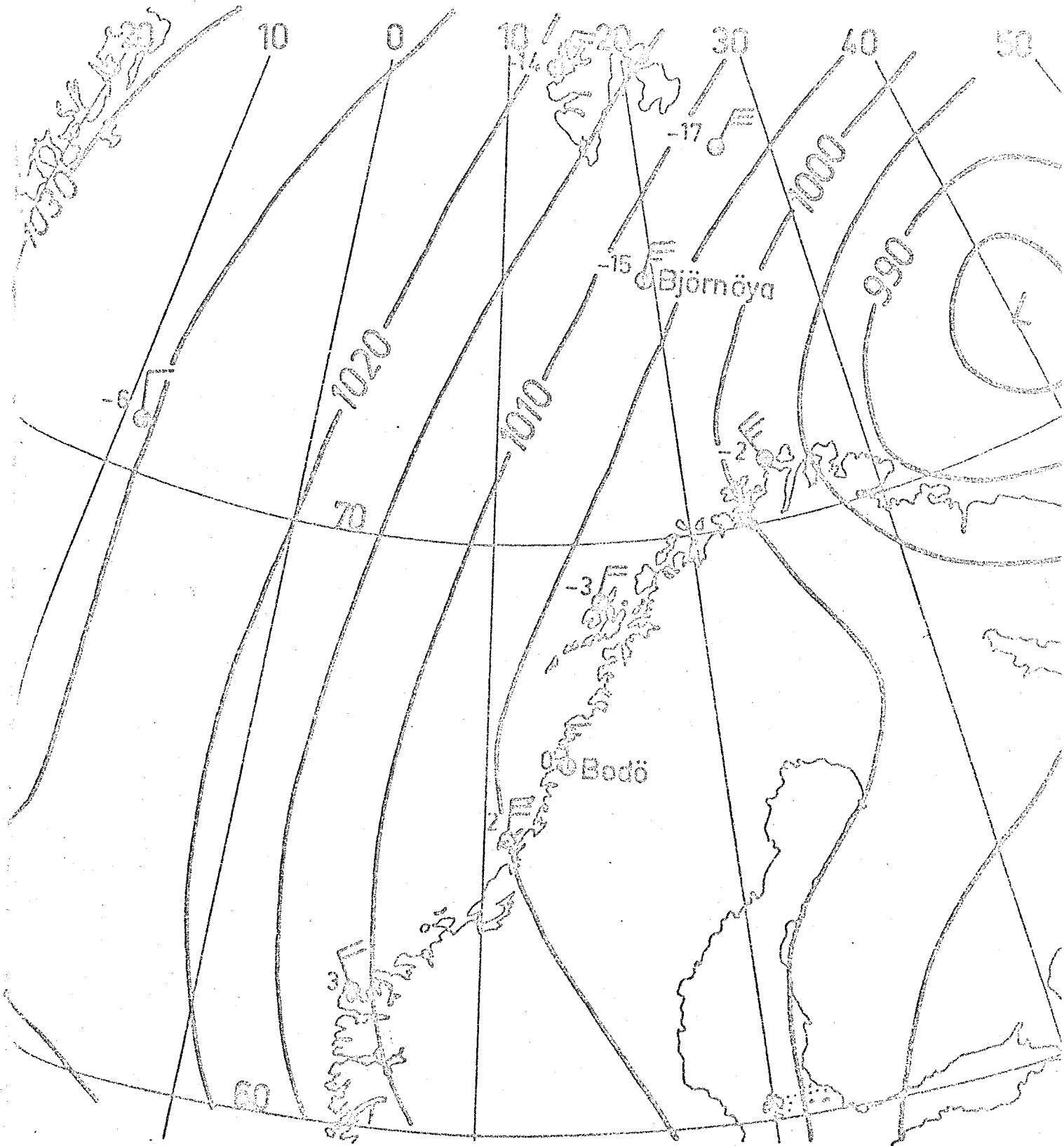


Fig. 1: Surface weather map for November 21, 1975, 12 GMT.

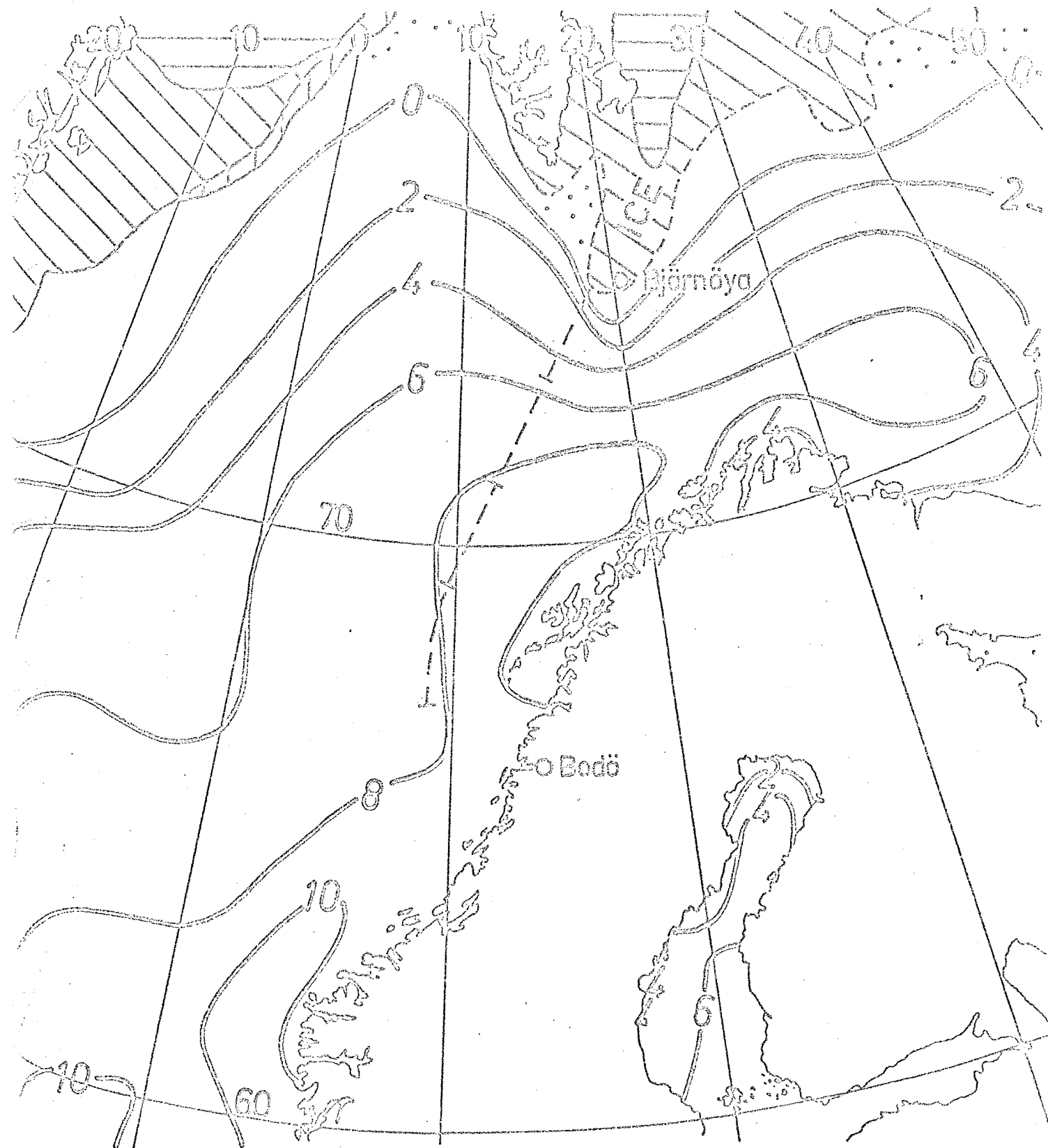


Fig. 2: Ocean surface temperature for November 20, 1975.

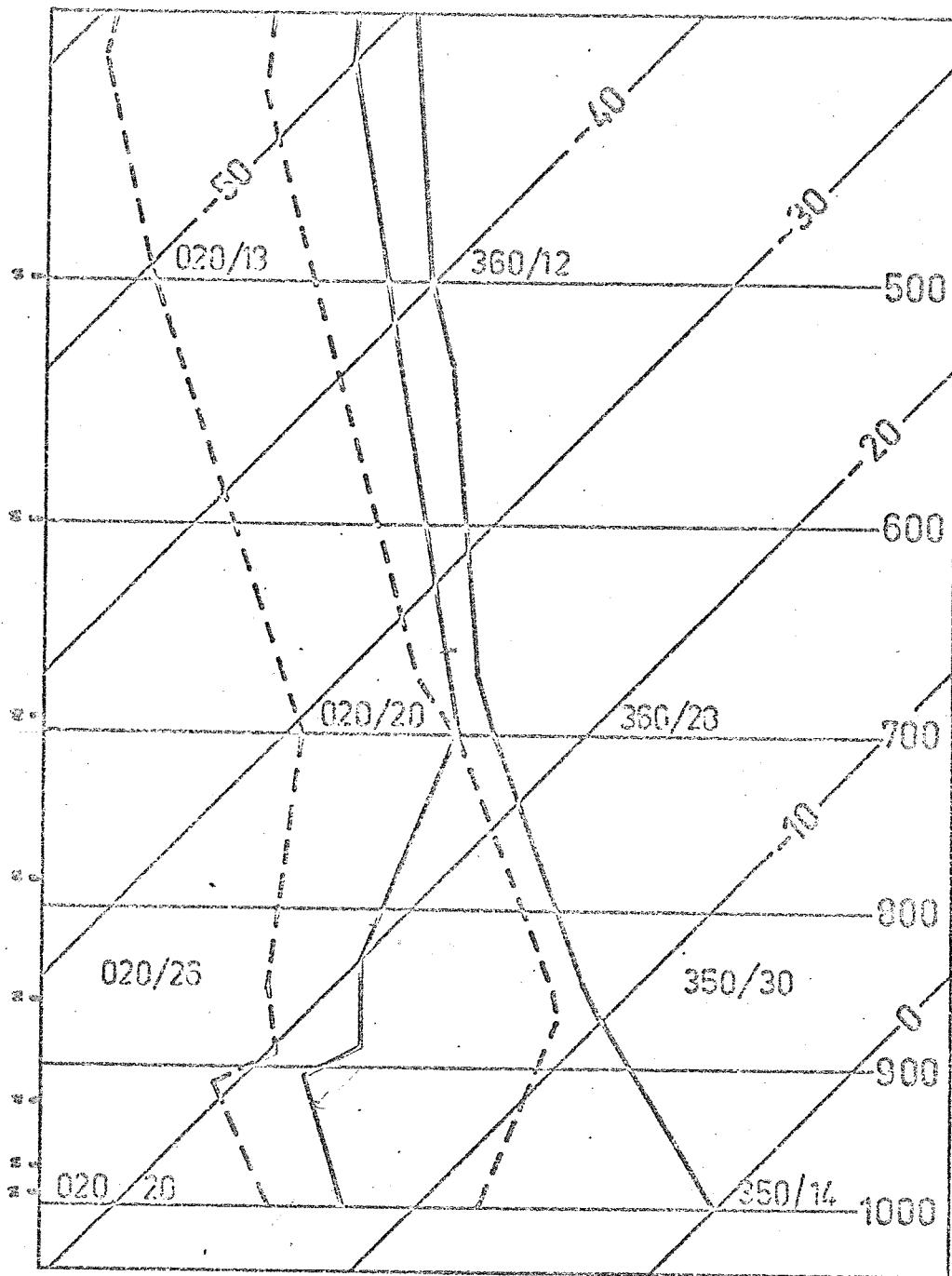


Fig. 3: Temperature and dew-point soundings for Björnöya and Bodö.

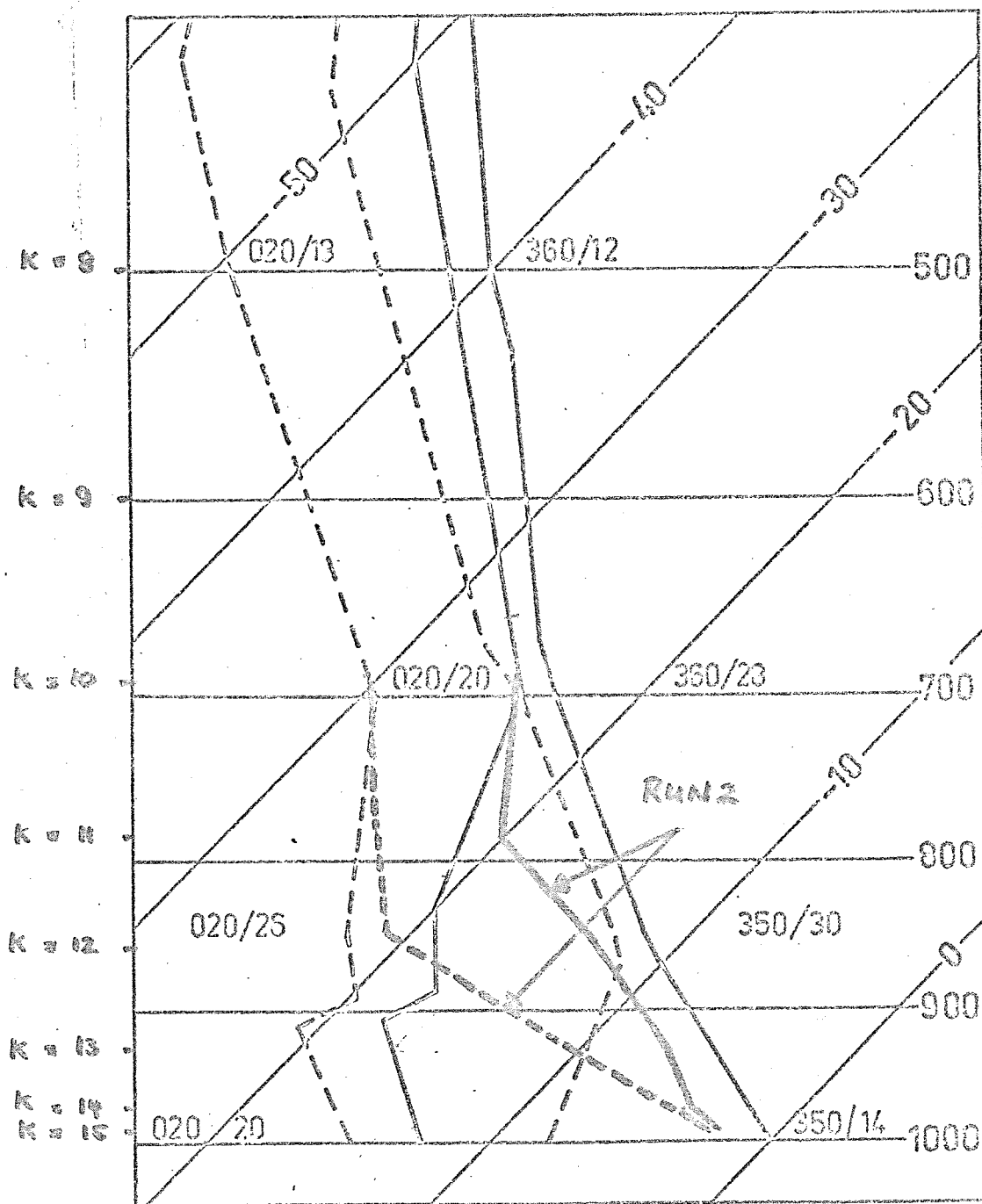
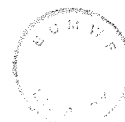


Fig. 4: Temperature and dew-point soundings for RUN 2, for Björnöya and Bodö.



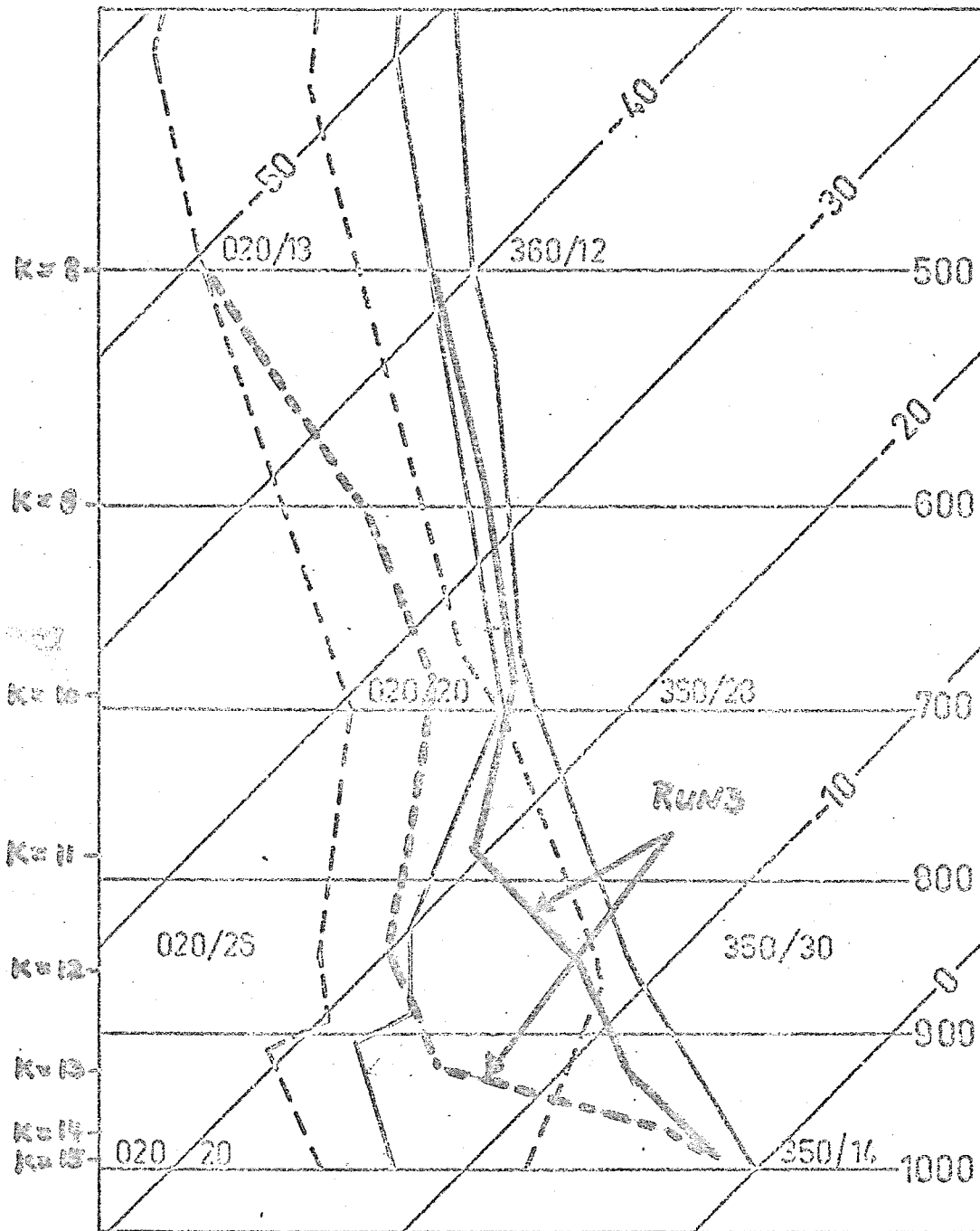


Fig. 5: Temperature and dew-point soundings for RUN 3, for Björnöya and Bodö.

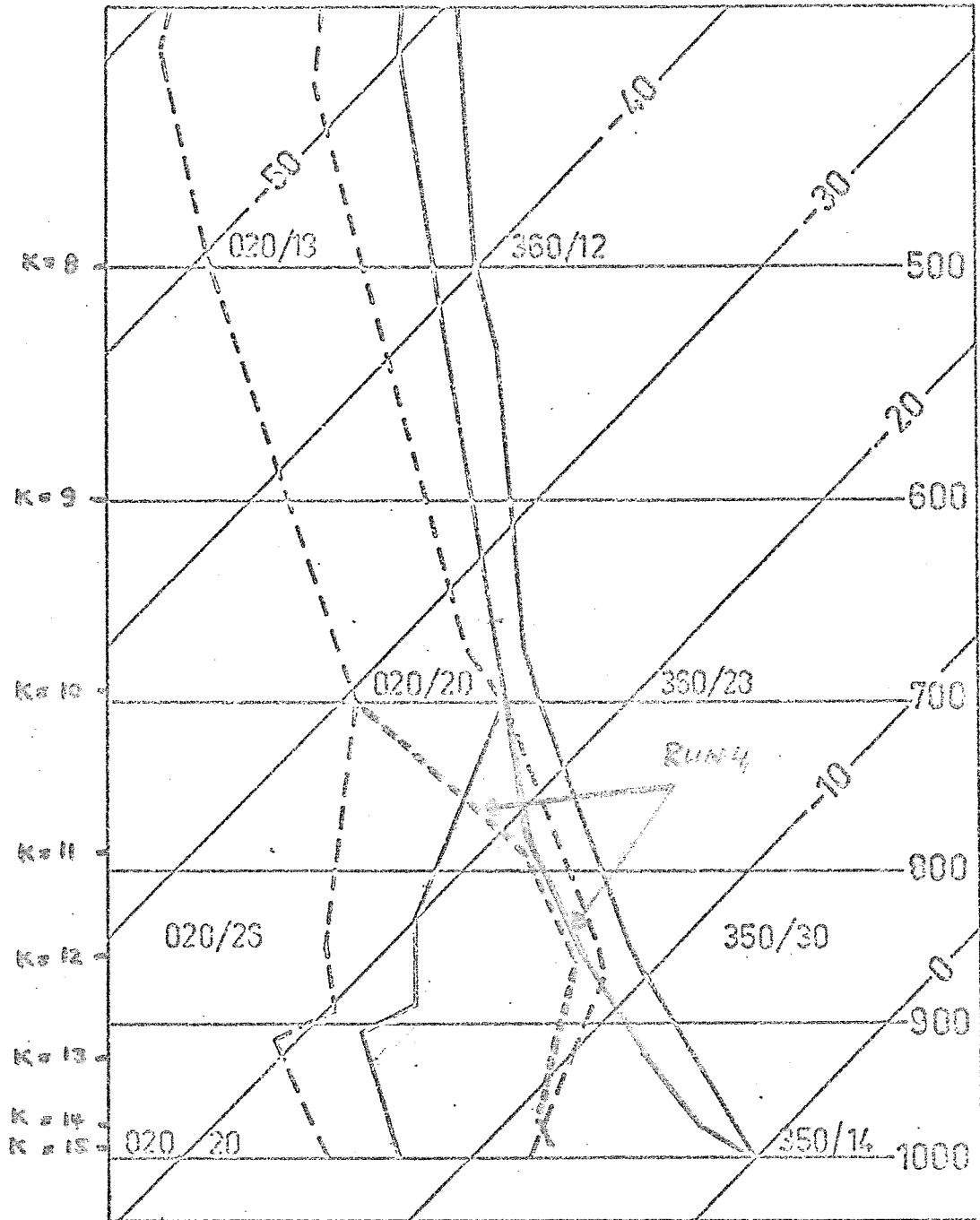


Fig. 6 : Temperature and dew-point soundings for RUN 4, for Björnöya and Bodö.

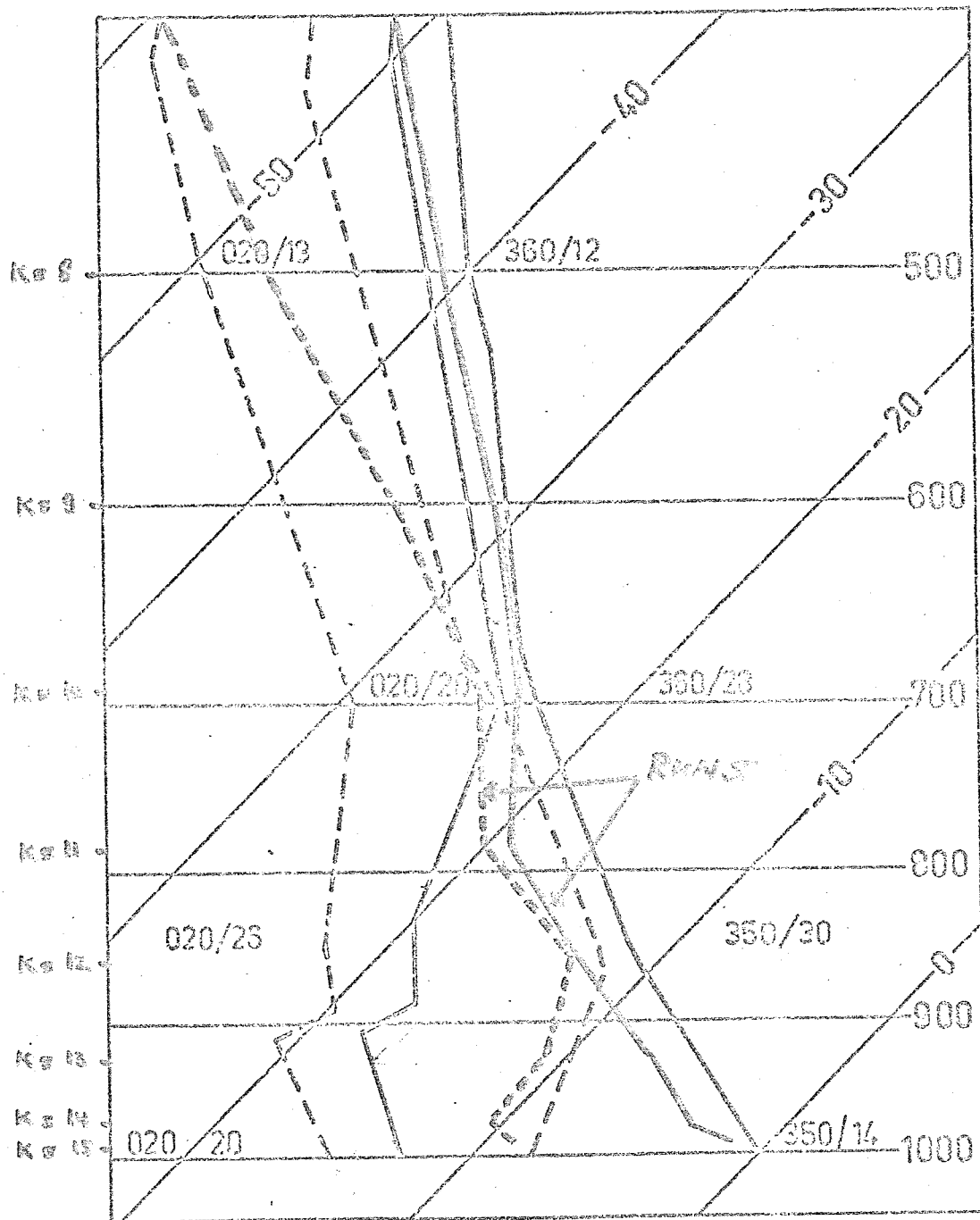


Fig. 7 : Temperature and dew-point soundings for RUN 5, for Björnöya and Bodö.

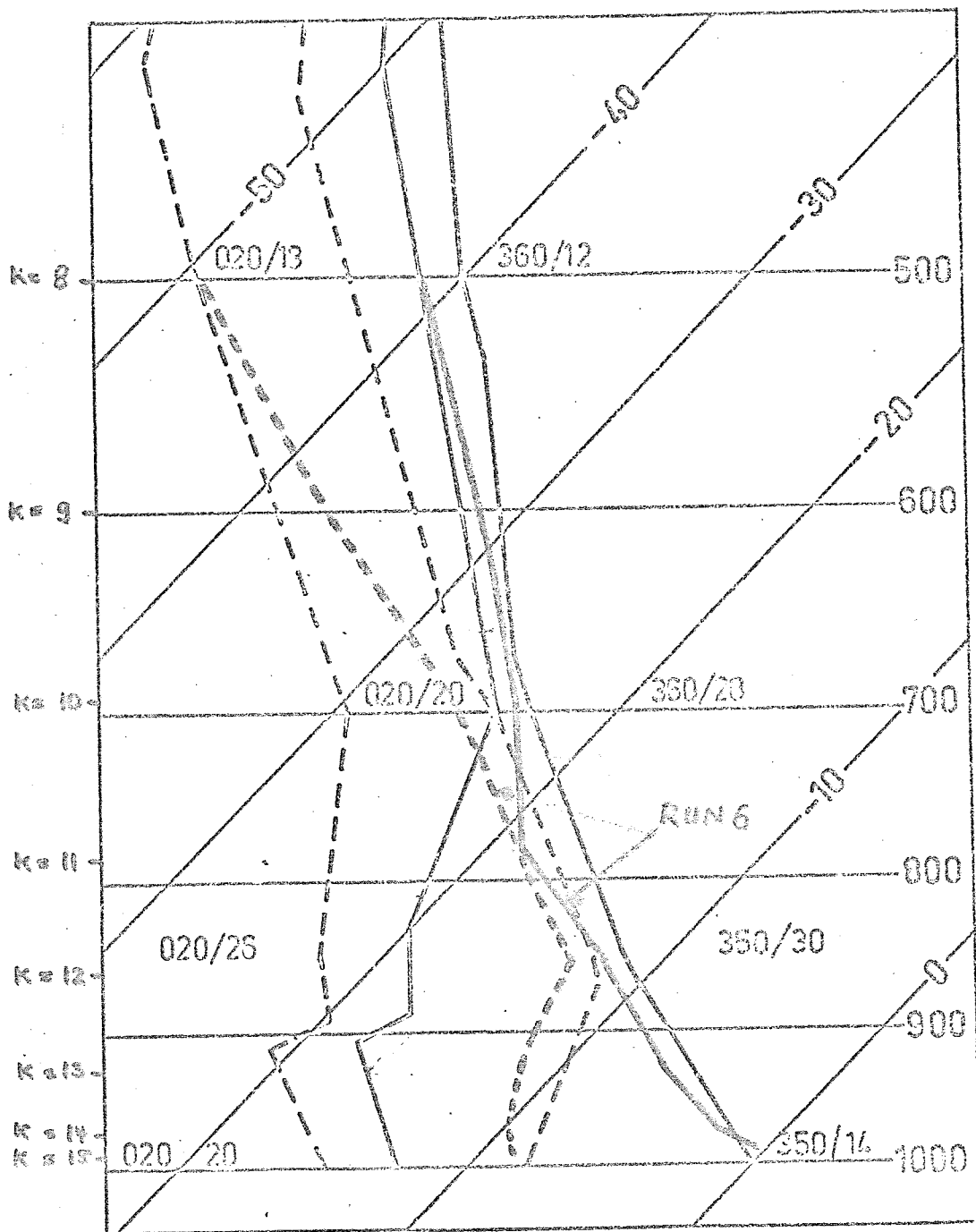


Fig. 8 : Temperature and dew-point soundings for RUN 6, for Björnøya and Bodø.